

# A variational quantum algorithm for Hamiltonian diagonalization

Jinfeng Zeng,<sup>1,\*</sup> Chenfeng Cao,<sup>1,†</sup> Chao Zhang,<sup>2</sup> Pengxiang Xu,<sup>2</sup> and Bei Zeng<sup>1,‡</sup>

<sup>1</sup>Department of Physics, The Hong Kong University of Science and Technology, Clear Water Bay, Kowloon, Hong Kong

<sup>2</sup>Peng Cheng Laboratory, Shenzhen, 518055, China

(Dated: April 8, 2022)

Hamiltonian diagonalization is at the heart of understanding physical properties and practical applications of quantum systems. It is highly desired to design quantum algorithms that can speedup Hamiltonian diagonalization, especially those can be implemented on near-term quantum devices. In this work, we propose a variational algorithm for Hamiltonians diagonalization (VQHD) of quantum systems, which explores the important physical properties, such as temperature, locality and correlation, of the system. The key idea is that the thermal states of the system encode the information of eigenvalues and eigenstates of the system Hamiltonian. To obtain the full spectrum of the Hamiltonian, we use a quantum imaginary time evolution algorithm with high temperature, which prepares a thermal state with a small correlation length. With Trotterization, this then allows us to implement each step of imaginary time evolution by a local unitary transformation on only a small number of sites. Diagonalizing these thermal states hence leads to a full knowledge of the Hamiltonian eigensystem. We apply our algorithm to diagonalize local Hamiltonians and return results with high precision. Our VQHD algorithm sheds new light on the applications of near-term quantum computers.

## I. INTRODUCTION

Naturally arising Hamiltonian of quantum systems exhibit local structure, which allows efficient algorithms on quantum computers to simulate the evolution of these systems. Diagonalizing these Hamiltonians, however, is a more challenging task for quantum computing, which also serves as important subroutines, for instance, of the celebrated Density Functional Theory (DFT) [1, 2] for important applications of quantum simulation in chemistry, materials sciences and technologies [3]. Quantum algorithms have been developed for finding the eigenvalues and eigenstates of Hamiltonians, for instance the one based on quantum fast Fourier transform [4]. However, implementing these algorithms require fault-tolerance [5], which are not expected to be achievable in the near future.

With the current Noise-Intermedia-Scale-Quantum (NISQ) era [6], it is highly desired to design quantum algorithms that can take advantage of the near-term quantum devices. Many variational/hybrid quantum algorithms are proposed in recent years, for tasks such as finding ground states of Hamiltonians (variational quantum eigen solver, VQE [7–9]), finding approximate solutions to combinatorial optimization problems (quantum approximate optimization algorithm QAOA [10]); diagonalizing density matrices of quantum systems (variational quantum state eigen solver, VQSE [11]; and variational quantum state diagonalization VQSD [12]), finding singular values of matrices [13], and training quantum Boltzmann machine (variational quantum Boltzmann machine [14,

15]). Along this line, the variational algorithm for finding Hamiltonian spectra has also been discussed [16], with also various new methods for finding excited states [17, 18].

In this work, we propose a new variational quantum algorithm for Hamiltonian diagonalization (VQHD) for quantum systems, which explores the important physical properties, such as temperature, locality and correlation, of the system. The key idea is that for any system Hamiltonian  $H$ , the thermal state  $\rho_\beta = e^{-\beta H} / \text{tr}(e^{-\beta H})$  encodes the information of the eigenvalues and eigenvectors of  $H$ , where  $\beta = 1/k_B T$  with  $T$  the temperature of the system. For small  $\beta$ ,  $\rho_\beta$  is full rank and diagonalizing  $\rho_\beta$  directly returns the eigensystem of  $H$ . Hence if we prepare the thermal state  $\rho_\beta$ , we can then use variational algorithms to diagonalize  $\rho_\beta$ , for obtaining the eigensystem of  $H$ .

To prepare the thermal state  $\rho_\beta$ , one can apply an imaginary time evolution with a thermofield double state, as proposed in [19]. The idea is illustrated in Fig. 1 (a), where each connected pair of dots represents a two-qubit maximally entangled state, and the initial thermofield double state  $|\text{TFD}(0)\rangle$  is hence a product of  $n$  entangled pairs. The imaginary time evolution  $e^{-\beta H/2}$  on  $|\text{TFD}(0)\rangle$  returns the state  $|\text{TFD}(\beta)\rangle$ , and  $\rho_\beta$  will be then obtained on the bottom  $n$  qubits by tracing out the top  $n$  qubits. For applying  $e^{-\beta H/2}$ , we choose a quantum imaginary time evolution (QITE) algorithm as proposed in [20]. An advantage of this choice is that, for small  $\beta$ , the many-body state  $\rho_\beta$  exhibits small correlation length, local unitary transformations on a relatively small size of local sites hence suffices to simulate the imaginary time evolution on a quantum computer.

We apply our algorithm for diagonalizing various local Hamiltonians, to obtain the full spectrum. Notice that a larger value of  $\beta$  can suppress high energy states

\* jfzeng@ust.hk

† chenfeng.cao@connect.ust.hk

‡ zengb@ust.hk

which will then return low-line eigenstates of  $H$ . Depending on the situation, our algorithm hence can also be applied to find low-lying states. Our method adds a new tool to the family of NISQ algorithms and will shed light on the near-term application of quantum computers.

## II. THE VARIATIONAL ALGORITHM FOR HAMILTONIAN DIAGONALIZATION

Consider a quantum system of  $n$  qubits. The system Hamiltonian  $H$  adopts the form

$$H = \sum_i H_i, \quad (2.1)$$

with each  $H_i$  acting nontrivially on geometrically local sites.

The thermal state  $\rho_\beta$  of the system has the form

$$\rho_\beta = \frac{e^{-\beta H}}{\text{tr}(e^{-\beta H})}, \quad (2.2)$$

where  $\beta = \frac{1}{k_B T}$ , where  $T$  is the temperature of the system.

Our variational quantum algorithm for Hamiltonian diagonalization (VQHD) involves the following two major steps:

- (S1) Prepare the thermal state  $\rho_\beta$  for small  $\beta$ .
- (S2) Diagonalize  $\rho_\beta$  to obtain the eigenvalues and eigenvectors of  $H$ .

There are various methods one can use for each (S1) and (S2). We discuss the details in the following.

### A. Preparation of $\rho_\beta$

The first major step (S1) of VQHD is to prepare quantum Gibbs state  $\rho_\beta$ , and to do so is known to be challenging [21]. There have been some proposed quantum algorithms to prepare the thermal state. Some of the methods are based on quantum sampling [22–24], which require quantum phase estimation as a subroutine, therefore are not suitable for NISQ devices.

There are also some variational algorithms proposed to be implemented on NISQ devices [14, 19, 25, 26]. The methods used in Refs [19, 25, 26] are based on minimizing the free energy of the system at certain temperature, which is challenging due to the nontrivial estimation of von Neumann entanglement entropy. Different authors use different approximation methods for the free energy estimation for running their algorithms on NISQ devices. However, these methods also introduce other degrees of complexity. Refs [26] approximately estimates the free energy with tools including quantum

amplitude estimation [27] and density matrix exponentiation [28, 29]. Refs [25] estimates the approximate free energy with a truncated Taylor series.

Two other proposals given in [14, 19] both start from the thermofield double (TFD) state and need to evolve in imaginary time on a quantum device. Ref. [19] argues that it is hard to implement quantum imaginary time evolution and design a variational time evolution between the origin Hamiltonian and interacted Hamiltonian, which also needs to approximately estimate the nontrivial free energy with Renyi entropy estimation [30]. While Ref. [14] straightforwardly employs a variational quantum imaginary time evolution [31, 32], which makes the algorithm much simpler. All those variational methods share the drawback that it is hard to design the variational ansatz space to include the target point and the barren plateaus effect [33] when using the gradient of loss in the quantum circuit.

The method starting from the TFD state and evolving in imaginary time for thermal state preparation is straightforward and simple, if we can implement the quantum imaginary time evolution (QITE) easily. Motta *et al.* [20] proposed an alternative QITE algorithm in addition to the variational one [31]. The QITE can be applied to determine ground state energy and the thermal average. We adopt this QITE algorithm to prepare the thermal state, which can take advantage of the small correlation length of the system in small  $\beta$ . Consequently, our method for preparing the thermal state  $\rho_\beta$  is to use the QITE algorithm given in [20] to evolve the TFD state as discussed in [19], and then trace out the subsystem of the TFD state.

Consider a  $2n$ -qubit pure state  $|\text{TFD}(0)\rangle$ , which is a maximally entangled state between the first  $n$  qubits (i.e. qubits  $1, 2, \dots, n$ ) and the other  $n$  qubits (i.e. qubits  $n+1, n+2, \dots, 2n$ ).

$$|\text{TFD}(0)\rangle = \sum_{i=1}^{2^n} |i\rangle |i\rangle, \quad (2.3)$$

where  $\{|i\rangle\}$  are the computational basis of  $n$  qubits. We now define the state

$$\begin{aligned} |\text{TFD}(\beta)\rangle &= \frac{e^{-\beta H/2}}{\sqrt{\text{tr}(e^{-\beta H})}} |\text{TFD}(0)\rangle \\ &= \frac{1}{\sqrt{\text{tr}(e^{-\beta H})}} \sum_{j=1}^{2^n} e^{-\beta h_j/2} |j\rangle |j\rangle, \end{aligned} \quad (2.4)$$

where  $\{|j\rangle\}$  are the orthonormal eigenvectors of  $H$ , and  $\{h_j\}$  are the corresponding eigenvalues. Tracing out the qubits  $n+1, n+2, \dots, 2n$  from  $|\text{TFD}(\beta)\rangle$  gives

$$\rho_\beta = \text{tr}_{n+1, n+2, \dots, 2n} |\text{TFD}(\beta)\rangle \langle \text{TFD}(\beta)|. \quad (2.5)$$

To be able to implement the quantum imaginary time evolution  $e^{-\beta H/2}$  on a quantum computer, we use a

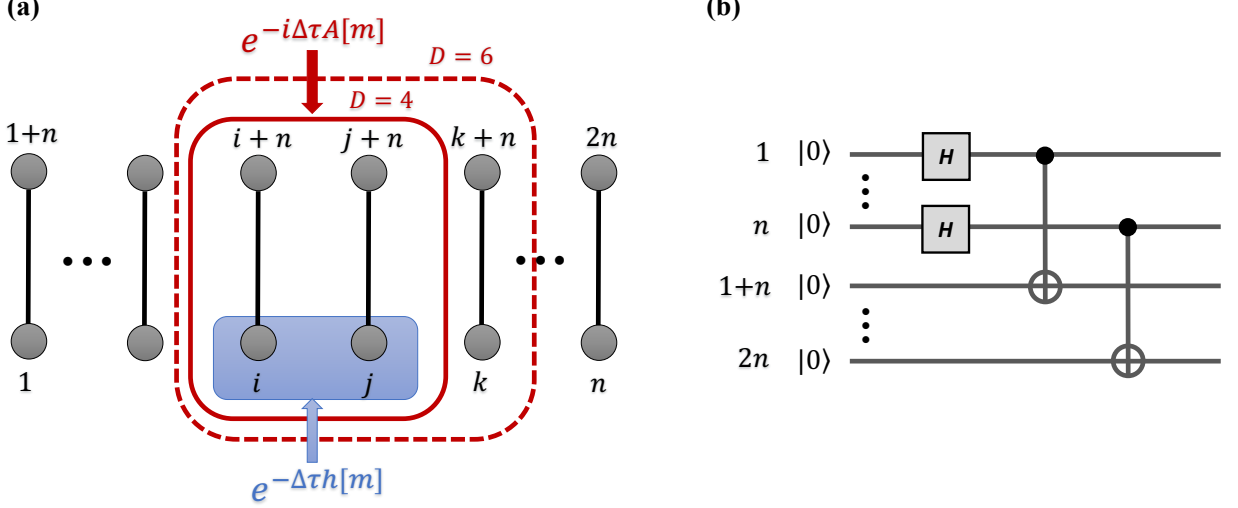


FIG. 1. (a) Schematic illustration of the basic idea of QITE algorithm and the locality of unitary evolution in QITE when apply to prepare the TFD state. The qubits from 1 to  $2n$  form an one dimension chain. The bond between  $i$  qubit and  $i+n$  qubit indicate the two qubit maximally entangled state  $(|00\rangle + |11\rangle)/\sqrt{2}$  on  $(i, i+n)$  qubits. And the one dimension chain represent the state  $|\text{TFD}(0)\rangle$  on 1 to  $2n$  qubits before apply the quantum imaginary time transformation. The blue shadow frame indicates the  $L$  ( $L = 2$ ) local imaginary time transformation  $e^{-\Delta\tau h[m]}$ , which can be reproduced by unitary transformation  $e^{-i\Delta\tau A[m]}$  acting on  $D \geq L$  qubit. When the  $L$  ( $L = 2$ ) local operator acting on  $(i, j)$  qubits inside the blue shadow frame, the  $D$  ( $D = 4$ ) qubit unitary operator act on  $(i, j, i+n, j+n)$  qubits indicated by the solid red box. When  $D = 6$  the unitary operator acting on  $(i, j, k, i+n, j+n, k+n)$  qubits indicated by the dotted red box. (b) The quantum circuit to prepare the state  $|\phi_0\rangle$  describe in the main text.

QITE algorithm as given in [20]. After Trotter decomposition of the corresponding imaginary time evolution in  $N = \frac{\beta/2}{\Delta\tau}$  steps, the basic idea of QITE is map the  $L$ -local non-unitary transformation to an approximate  $D$  local unitary transformation in each step,

$$|\psi'\rangle = \frac{1}{\sqrt{c}} e^{-\Delta\tau h[m]} |\psi\rangle \approx e^{-i\Delta\tau A[m]} |\psi\rangle, \quad (2.6)$$

where  $c = \langle \psi | e^{-2\Delta\tau h[m]} | \psi \rangle$  is the normalization factor. Each  $h[m]$  acts nontrivially on  $L$  qubits.  $A[m]$  is Hermitian and act on  $D$  qubits.  $A[m]$  can be expanded in terms of Pauli basis on  $D$  qubits,

$$A[m] = \sum_{i_1 i_2 \dots i_D} a[m]_{i_1 i_2 \dots i_D} \sigma_{i_1} \sigma_{i_2} \dots \sigma_{i_D} = \sum_I a[m]_I \sigma_I \quad (2.7)$$

where  $a[m]_I$  is the coefficient of combine Pauli operator  $\sigma_I$  and the index  $I$  is a combination of qubit indexes  $\{i_1, i_2, \dots, i_D\}$ . To find coefficients  $a[m]_I$  and determine the concrete form of  $A[m]$ , we minimize the function

$$\| |\psi'\rangle - (1 - i\Delta\tau A[m]) |\psi\rangle \|, \quad (2.8)$$

which is consistent with our goals as described in Eq. (2.6). It can be easily derived that the solution of

the minimization is subject to the linear equation,

$$(S + S^T) \mathbf{a}[m] = -\mathbf{b}, \quad (2.9)$$

Where the matrix  $S$  and vector  $\mathbf{b}$  can be obtained by  $D$  local measurements on the  $|\psi\rangle$ ,

$$S_{IJ} = \langle \psi | \sigma_I^\dagger \sigma_J | \psi \rangle, \\ b_I = -2\text{Im} \left[ \frac{1}{\sqrt{c}} \langle \psi | \sigma_I^\dagger h[m] | \psi \rangle \right],$$

where  $\text{Im}[\cdot]$  means the imaginary part of the variable inside. After solve the linear equation in the classical computer, we get the  $\mathbf{a}[m]$  and construct a quantum circuit to implement the unitary transformation  $e^{-i\Delta\tau A[m]} |\psi\rangle$  on NISQ quantum devices at each step.

One of the most import parameters of the QITE algorithm is  $D$ , which is the number of qubits that the local unitary transformation acts on. Given  $L$  local Hamiltonian, the QITE algorithm can capture the correlation of the original Hamiltonian only if  $D \geq L$ . However, our goal is to prepare the thermofield double state  $|\text{TFD}(\beta)\rangle$  start from  $|\text{TFD}(0)\rangle$ , which is a maximally entangled state between the first  $n$  qubits and the other. When the unitary local operator act on  $i$  qubit, it must include the  $i+n$  qubit and  $D \geq 2L$ . In this paper, we consider the 2 local Hamiltonian and  $D \geq 4$ . The locality of the  $D$

qubit unitary operator in QITE algorithm is shown in Fig. 1 (a) with  $L = 2$ ,  $D = 4$  and  $D = 6$ .

Notes that the thermofield double state  $|\text{TFD}(0)\rangle$  is not normalized. We define a variable

$$|\phi_0\rangle = \frac{1}{\sqrt{2^n}} |\text{TFD}(0)\rangle = \frac{1}{\sqrt{2^n}} \sum_{i=1}^{2^n} |i\rangle|i\rangle. \quad (2.10)$$

The  $|\phi_0\rangle$  is normalization and can be easily prepared with a quantum circuit. Fig. 1 (b) shows the quantum circuit to prepare the state  $|\phi_0\rangle$ : start with the initial state  $|0\rangle^{\otimes 2n}$  and apply Hadamard gates on qubits from 1 to  $n$ ; then apply the CNOT gates on  $(i, i+n)$  qubits, where  $i$  is the control qubit and  $i+n$  is the target qubit and  $i$  run over 1 to  $n$ . After preparing the initial state  $|\phi_0\rangle$  by a quantum circuit, we use the QITE algorithm to obtain

$$|\text{TFD}(\beta)\rangle = \sqrt{\frac{2^n}{\text{tr}(e^{-\beta H})}} e^{-\beta H/2} |\phi_0\rangle. \quad (2.11)$$

### B. Diagonalization of $\rho_\beta$

The second major step (S2) of VQHD is to diagonalize  $\rho_\beta$  for obtaining the eigenvalues and eigenvectors of  $\rho_\beta$ . In general, for any quantum state  $\rho$ , quantum principle component analysis [28] can be used to diagonalize  $\rho$  with an exponential speedup compared to classical computers. However, this method needs fault-tolerance hence it cannot be implemented on NISQ devices. Variational Quantum State Diagonalization (VQSD) [12] and Variational Quantum State Eigensolver (VQSE) [11] are alternative algorithms to extract the eigenvalues and eigenstates of  $\rho$ , and they can be used on near-term devices. Compared with VQSD, VQSE needs less number of qubits. Here we then use VQSE for diagonalizing  $\rho_\beta$ .

After preparing the thermal state  $\rho_\beta$  with QITE, we train a parameterized quantum circuit  $V(\theta)$  to partially diagonalize it with VQSE. Denote the circuit output state as  $\rho_f$ ,  $\rho_f = V(\theta)\rho_\beta V^\dagger(\theta)$ . Suppose we want to obtain the lowest  $K$  eigenstates of  $H$ , the cost Hamiltonian is therefore

$$H_{\text{cost}} \equiv \mathbb{1} - \sum_{i=1}^K q_i |i\rangle\langle i|, \quad (2.12)$$

where  $q_i > q_{i+1}$  for  $1 \leq i \leq K-1$ . We measure the expectation value of  $\rho_f$  on the cost Hamiltonian to estimate the cost function

$$C(\theta) = \text{Tr} [H_{\text{cost}} \rho_f], \quad (2.13)$$

then optimize the parameters  $\theta$  to minimize it.

$\rho_\beta$  and  $H$  share the same eigenstates.  $\rho_\beta$  of a non-degenerate Hamiltonian is also non-degenerate, reaching the minimum value of  $C(\theta)$  indicates an exact par-

tial diagonalization of the  $\rho_\beta$ . Denote the eigenstates of  $H$  as  $\{|\psi_k\rangle\}$ , where  $k$  is the level index.  $V(\theta)|\psi_k\rangle = |k\rangle$  for exact partial diagonalization with  $k \leq K$ , we can run the inverse of  $V(\theta)$  to prepare the lowest  $K$  eigenstates of  $H$ , measurements of  $H$  give the corresponding eigenvalues.

$$\langle \psi_k | H | \psi_k \rangle = \lambda_k. \quad (2.14)$$

## III. RESULTS

We implement the VQHD algorithm to demonstrate its feasibility. We apply our the algorithm to diagonalize two one-dimensional Hamiltonian, the random 2-local Hamiltonian and the random transverse field Heisenberg Hamiltonian with periodic boundary condition.

The one-dimensional random 2-local Hamiltonian is defined as

$$\begin{aligned} H_{\text{R2L}} &= \sum_{\langle ij \rangle} h[i] \cdot \sigma[i, j] \\ &= \sum_{\langle ij \rangle} \sum_I^{16} h_I[i] \sigma_I[i, j] \\ &= \sum_{\langle ij \rangle} \sum_{\alpha=1}^4 \sum_{\beta=1}^4 h_{\alpha\beta}[i] \sigma_\alpha[i] \sigma_\beta[j], \end{aligned} \quad (3.1)$$

where  $\langle ij \rangle$  denote the summation over the nearest-neighbor (NN) lattice site.  $\alpha, \beta$  denote the Pauli operator index and  $\sigma_\alpha[i]$  is one of the Pauli operators ( $\sigma_0 = I, \sigma_1 = X, \sigma_2 = Y, \sigma_3 = Z$ ) act on site  $i$ . The coefficient  $h_{\alpha\beta}[i]$  is sampling from a uniform distribution over the interval  $[0, 1)$  and subject to the condition  $\sum_{\alpha\beta} h_{\alpha\beta}[i] = 16n$ , where  $n$  is the number of lattice sites.

The one-dimensional Heisenberg Hamiltonian with random transverse field is defined as

$$H_{\text{RTH}} = \sum_{\langle ij \rangle} \mathbf{S}_i \cdot \mathbf{S}_j + \sum_i^n h_i Z_i \quad (3.2)$$

where  $\langle ij \rangle$  denote the summation over the nearest-neighbor (NN) lattice site.  $h_i$  is the coefficient of the transverse field term on each site, which is sampling from a uniform distribution over the interval  $[0, 1)$  and subject to the condition  $\sum_i h_i = n$ , where  $n$  is the number of lattice sites.

### A. The numerical results for the preparation of $\rho_\beta$

In the part we discuss the numerical results of preparation of  $\rho_\beta$ . As discussed in Section II A, the minimum  $D$  is 4 for preparing  $\rho_\beta$ . In all the experiments we set  $D = 4$ .

The results of the random 2-local Hamiltonian and



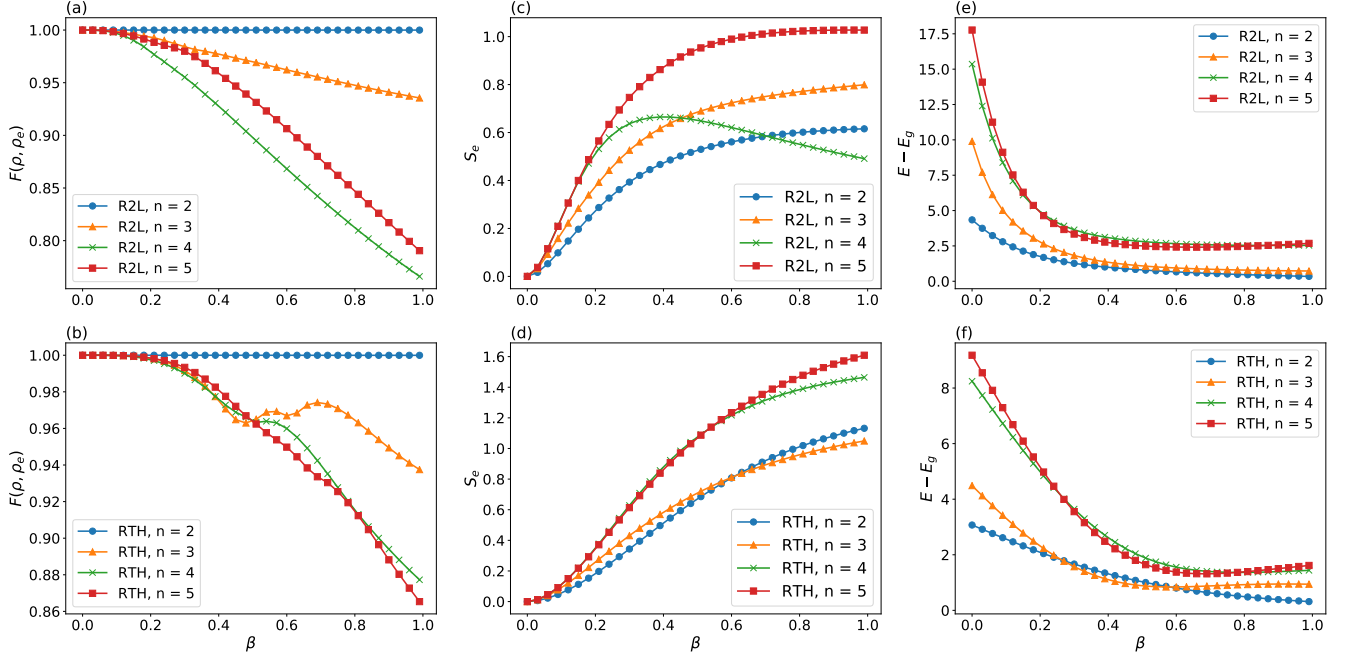


FIG. 2. The numerical results of preparation of  $\rho_\beta$  for random 2-local Hamiltonian and the random transverse field Heisenberg Hamiltonian with  $D = 4$ . The fidelity between the  $\rho$  procured by QITE and the exact  $\rho_0$  as a function of  $\beta$  for (a) random 2-local Hamiltonian and (b) random transverse field Heisenberg Hamiltonian. The von Neumann entropy for the exact state  $|\psi_{CD}\rangle$  calculated by Eq. 2.11 for (c) random 2-local Hamiltonian and (d) random transverse field Heisenberg Hamiltonian. The C subsystem include the sites  $(1, 2, \dots, n/2, 1+n, 2+n, \dots, n/2+n)$ . The relative energy  $E - E_g$  between the energy calculated by QITE and the ground state energy  $E_g$  as a function of  $\beta$  respectively for (e) random 2-local Hamiltonian and (f) random transverse field Heisenberg Hamiltonian.

the random transverse field Heisenberg Hamiltonian are summarized in Fig. 2. To characterize how well the QITE can prepare the target state  $\rho_\beta$ , Fig. 2 (a) and (b) shows  $F(\rho, \rho_e) = (\text{tr} \sqrt{\sqrt{\rho} \rho_e \sqrt{\rho}})^2$ , the fidelity between the  $\rho$  produced by QITE and the exact  $\rho_e$  as a function of  $\beta$  respectively for (a) random 2-local Hamiltonian and (b) random transverse field Heisenberg Hamiltonian. When the Hamiltonian defined on  $n = 2$  site, the whole  $|\text{TFD}(\beta)\rangle$  defined on  $2n = 4$  qubits. If we set  $D = 4$ , the unitary operator act on the whole system and can capture the correlation of system. The fidelity  $F(\rho, \rho_e)$  of  $n = 2$  is approximated to 1 in all  $\beta$  as shown in the blue point line in Fig. 2 (a) and (b). When  $n > 2$  the fidelity  $F(\rho, \rho_e)$  decrease as  $\beta$  increase. However, the fidelity  $F(\rho, \rho_e)$  still approximate 1 for  $\beta < 0.1$  and state produced by QITE preform well in small  $\beta$ . This could be understood as follows, for small  $\beta$  the many body state  $\rho_\beta$  is near the initial  $\rho_0$  and exhibit small correlation. Fig. 2 (c) and (d) show the von Neumann entropy  $S_e = -\text{tr} \rho_C \log \rho_C$  for the exact state  $|\psi_{CD}\rangle$  calculated by the Eq. 2.11 respectively for (c) random 2-local Hamiltonian and (d) random transverse field Heisenberg Hamiltonian. The C subsystem include the sites  $(1, 2, \dots, n/2, 1+n, 2+n, \dots, n/2+n)$ . The entropy  $S_e = 0$  at  $\beta = 0$  and the entropy increase as  $\beta$  increase. The unitary act only  $D = 4$  qubits can approx-

imate the small correlation of the original Hamiltonian for small  $\beta$ , but can not capture the correlation for large  $\beta$ .

Note that when applying for the QITE to solve the ground state energy problem. We need large  $\beta$  and large  $D$  for big  $n$ . Fig. 2 (e) and (f) shown the relative energy  $E - E_g$  between the energy calculated by QITE and the ground state energy  $E_g$  respectively for (e) random 2-local Hamiltonian and (f) random transverse field Heisenberg Hamiltonian. As  $\beta$  increase to 1, the relative energy are convergent for all  $n$ . But only the energy of  $n = 2$  converges to ground state energy. The relative energy  $E - E_g$  is large for large  $n$ . Compare to the ground state problem, we need a small  $D$  and small  $\beta$  to prepare the  $\rho$  when apply for the QITE algorithm. As space and time cost of QITE are proportional to exponentials in  $D$ . The number of measurements is also bounded by  $e^D$ . Hence, we reduce the time and space cost as well as the number of measurements.

## B. The numerical results for the diagonalization of $\rho_\beta$

After preparing  $\rho_\beta$  for the random 2-local Hamiltonian and the random transverse field Heisenberg Hamiltonian with high fidelity, we apply VQSE to find

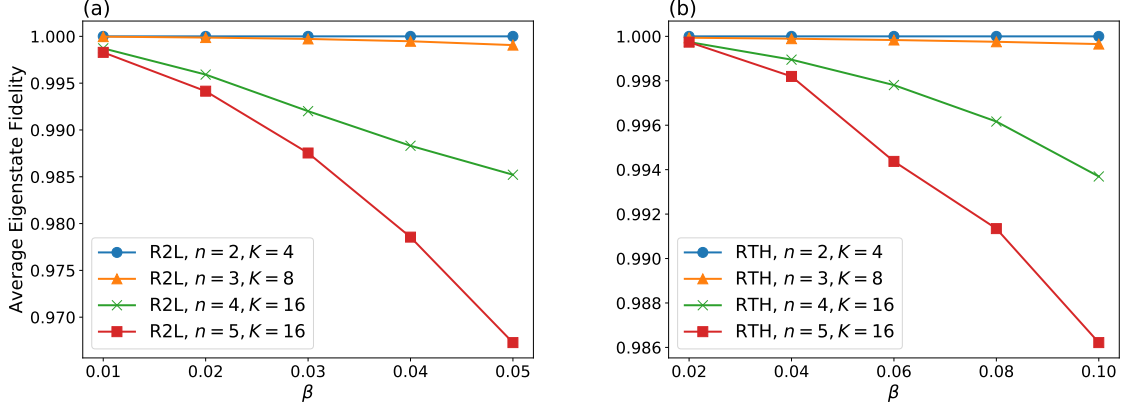


FIG. 3. The average fidelity between the predicted  $K$  eigenstates and the real lowest  $K$  eigenstates of  $H$  for (a) random 2-local Hamiltonian  $H$  with and (b) random transverse field Heisenberg Hamiltonian. The performance of VQHD declines as  $n$  and  $\beta$  increase. But for small  $\beta$ , VQHD always performs well.

the lowest  $K$  eigenstates of  $H$ , i.e. the highest  $K$  eigenstates of  $\rho_\beta$  if  $\rho_\beta$  is exactly prepared. After training, we calculate the average fidelity for the  $K$  target eigenstates.

The parameterized quantum circuits can be trained by non-gradient methods (e.g. Nelder-Mead method) or gradient descent methods. Here we use the latter one. Although the gradient will vanish exponentially as  $n$  increase [33], there are several methods to suppress the phenomenon, such as selecting special initial parameters [34], replacing the global cost function by a local cost function [35], training the circuit with an adaptive Hamiltonian [11].

The results for two Hamiltonian are shown in Fig. 3. We exactly diagonalize  $\rho_\beta$  for  $n = 2, 3, 4$ , partially diagonalize  $\rho_\beta$  for  $n = 5$ . A small  $K$  that satisfies  $K \ll 2^n$  makes the training much easier. VQSE performs well for small  $\beta$  cases, the performance reduction for large  $\beta$  is due to the inexact preparation of  $\rho_\beta$ .

#### IV. DISCUSSION

In this work, we proposed a variational algorithm for diagonalizing many-body Hamiltonians. Our VQHD method explores important physical properties of local Hamiltonians, including temperature, locality and correlation.

The key idea is that the thermal state  $\rho_\beta = e^{-\beta H} / \text{tr}(e^{-\beta H})$  encodes the information of eigenvalues and eigenstates of  $H$ , for any  $\beta$  in principle. Due to the exponential function, larger  $\beta$  will suppress high energy states, hence to retrieve information of low-lying states of  $H$ . Diagonalizing  $\rho_\beta$  with a variational algorithm on a quantum computer will then result in either full spectrum or low-lying eigenstates of  $H$ , depending on  $\beta$ .

$\rho_\beta$  can be obtained from the thermofield double state  $|\text{TFD}(\beta)\rangle = e^{-\beta H/2} |\text{TFD}(0)\rangle$ , by replacing the imagi-

nary time evolution  $e^{-\beta H/2}$  with a unitary transformation implemented on a quantum computer. For small  $\beta$ , the many-body state  $|\text{TFD}(\beta)\rangle$  has a small correlation length. With Trotterization of the imaginary time evolution  $e^{-\beta H/2}$ , each step can hence be replaced by a unitary transformation on only a small number of sites.

The main reason that we choose the QITE proposed in [20] instead of the variational one [31] in our variational quantum algorithm of Hamiltonian diagonalization is that we only need to consider the small  $\beta$  region and the local unitary transformation only needs to involve a small number of qubits. To solve the ground state energy, however, the QITE algorithm needs a larger number of qubits in each step of the unitary transformation. In principle, starting from an initial state that has some overlap with the ground state, evolve imaginary time to infinity large  $\beta$  can converges to the ground state. In practice, we need a larger  $\beta$  and  $D$  for the ground-state problem than thermal state preparation in QITE. We hence save the space and time cost of QITE algorithm when applying to the preparation of thermal states. Another significant difference between the thermal state preparation and the ground state problem is the locality of the unitary operators in QITE. We say that the TFD state has a smaller correlation length for small  $\beta$ , which is just defined on the first  $n$  qubits. Note that, the initial state  $|\text{TFD}(0)\rangle$  is a maximally entangle state between the first  $n$  qubits and final  $n$  qubits. The unitary transformations must capture the correlations between the  $i$  and  $i + n$  qubits, hence always need to include the pair  $(i, i + n)$  in the  $D$  qubits unitary transformations.

#### ACKNOWLEDGEMENT

PX thanks the support by the Key-Area Research and Development Program of Guangdong Province (No.2019B121204008).

- 
- [1] P. Hohenberg and W. Kohn, *Phys. Rev.* **136**, B864 (1964).
  - [2] W. Kohn and L. J. Sham, *Phys. Rev.* **140**, A1133 (1965).
  - [3] T. E. Baker and D. Poulin, [arXiv:2008.05592](#) (2020).
  - [4] D. S. Abrams and S. Lloyd, *Phys. Rev. Lett.* **83**, 5162 (1999).
  - [5] F. Gaitan, *Quantum error correction and fault tolerant quantum computing* (CRC Press, 2008).
  - [6] J. Preskill, *Quantum* **2**, 79 (2018).
  - [7] A. Peruzzo, J. McClean, P. Shadbolt, M.-H. Yung, X.-Q. Zhou, P. J. Love, A. Aspuru-Guzik, and J. L. O'Brien, *Nature communications* **5**, 4213 (2014).
  - [8] J. R. McClean, J. Romero, R. Babbush, and A. Aspuru-Guzik, *New Journal of Physics* **18**, 023023 (2016).
  - [9] A. Kandala, A. Mezzacapo, K. Temme, M. Takita, M. Brink, J. M. Chow, and J. M. Gambetta, *Nature* **549**, 242 (2017).
  - [10] E. Farhi, J. Goldstone, and S. Gutmann, [arXiv:1411.4028](#) (2014).
  - [11] M. Cerezo, K. Sharma, A. Arrasmith, and P. J. Coles, [arXiv:2004.01372](#) (2020).
  - [12] R. LaRose, A. Tikku, É. O'Neel-Judy, L. Cincio, and P. J. Coles, *npj Quantum Information* **5**, 57 (2019).
  - [13] C. Bravo-Prieto, D. Garcia-Martin, and J. Latorre, *Phys. Rev. A* **101**, 062310 (2020).
  - [14] C. Zoufal, A. Lucchi, and S. Woerner, [arXiv:2006.06004](#) (2020).
  - [15] Y. Shingu, Y. Seki, S. Watabe, S. Endo, Y. Matsuzaki, S. Kawabata, T. Nikuni, and H. Hakoshima, [arXiv:2007.00876](#) (2020).
  - [16] T. Jones, S. Endo, S. McArdle, X. Yuan, and S. C. Benjamin, *Phys. Rev. A* **99**, 062304 (2019).
  - [17] O. Higgott, D. Wang, and S. Brierley, *Quantum* **3**, 156 (2019).
  - [18] K. M. Nakanishi, K. Mitarai, and K. Fujii, *Phys. Rev. Research* **1**, 033062 (2019).
  - [19] J. Wu and T. H. Hsieh, *Phys. Rev. Lett.* **123**, 220502 (2019).
  - [20] M. Motta, C. Sun, A. T. Tan, M. J. O'Rourke, E. Ye, A. J. Minnich, F. G. Brandão, and G. K.-L. Chan, *Nature Physics* **16**, 205 (2020).
  - [21] D. Aharonov, I. Arad, and T. Vidick, [arXiv:1309.7495](#).
  - [22] K. Temme, T. J. Osborne, K. G. Vollbrecht, D. Poulin, and F. Verstraete, *Nature* **471**, 87 (2011).
  - [23] D. Poulin and P. Wocjan, *Phys. Rev. Lett.* **103**, 220502 (2009).
  - [24] M.-H. Yung and A. Aspuru-Guzik, *Proceedings of the National Academy of Sciences* **109**, 754 (2012).
  - [25] Y. Wang, G. Li, and X. Wang, [arXiv:2005.08797](#).
  - [26] A. N. Chowdhury, G. Hao Low, and N. Wiebe, [arXiv:2002.00055](#).
  - [27] G. Brassard, P. Hoyer, M. Mosca, and A. Tapp, [arXiv:quant-ph/0005055](#).
  - [28] S. Lloyd, M. Mohseni, and P. Rebentrost, *Nature Physics* **10**, 631 (2014).
  - [29] G. Hao Low and I. L. Chuang, [arXiv:1610.06546](#).
  - [30] R. Islam, R. Ma, P. M. Preiss, M. Eric Tai, A. Lukin, M. Rispoli, and M. Greiner, *Nature* **528**, 77 (2015).
  - [31] S. McArdle, T. Jones, S. Endo, Y. Li, S. C. Benjamin, and X. Yuan, *npj Quantum Information* **5**, 75 (2019).
  - [32] X. Yuan, S. Endo, Q. Zhao, Y. Li, and S. Benjamin, [arXiv:1812.08767](#).
  - [33] J. R. McClean, S. Boixo, V. N. Smelyanskiy, R. Babbush, and H. Neven, *Nature Communications* **9**, 4812 (2018).
  - [34] E. Grant, L. Wossnig, M. Ostaszewski, and M. Benedetti, *Quantum* **3**, 214 (2019).
  - [35] M. Cerezo, A. Sone, T. Volkoff, L. Cincio, and P. J. Coles, [arXiv:2001.00550](#) (2020).